Desalination and Water Treatment
www.deswater.com

doi: 10.5004/dwt.2019.23544

144 (2019) 89–98
March

Experimental development of contaminants removal from multicomponent solutions using ZVI, zeolite and modified construction aggregate – batch and column tests

Katarzyna Pawluk*, Joanna Fronczyk, Kazimierz Garbulewski

Faculty of Civil and Environmental Engineering, Department of Geotechnical Engineering, Warsaw University of Life Sciences–SGGW, Nowoursynowska 159, Warsaw 02-787, Poland; emails: katarzyna_pawluk@sggw.pl (K. Pawluk), joanna_fronczyk@sggw.pl (J. Fronczyk), kazimierz_garbulewski@sggw.pl (K. Garbulewski)

Received 22 January 2018; Accepted 28 November 2018

ABSTRACT

The aim of this study was to examine the ability of zero-valent iron (ZVI), zeolite (Z) and modified construction aggregate (MCA) to remove heavy metals from aqueous solutions. In addition, the use of an alternative material in permeable reactive barriers (PRBs) technology was investigated. This paper presents the premilary kinetic batch test and continuous-flow column test results by single- and multi-layered systems. The batch tests were conducted using 2.0 g of materials with 100 mL of solution (PE flask) with a constant concentration of heavy metals (30 mg/L). The flasks were sealed and placed in a rotary shaker at 15 rpm at the room temperature of 21°C ± 2°C; the concentrations of metal ions were measured in time spans (1, 3, 6, 10, 24 and 48 h) to determine the removal ratio. During the contact with Z, the removal of Pb(II) was on average 88% and for other metals was at approximately 20%. The efficiency of Ni, Pb and Cu removal on MCA was higher than 90%, while on ZVI all metals were practically completely removed. In column tests, after the saturation of materials beds, the evaluation of hydrodynamic parameters of the materials was performed by adding a pulse dose of chloride solution as a mobile tracer. The amount of adsorption was determined by conducting the column test for a synthetic multicomponent model solution (20 mg/L of Cd, Cu, Ni, Pb and Zn), where at intervals the heavy metal concentrations were analysed. The breakthrough time (t_{bR}) for Cd was in the range of 2.93×10^6 s for MCA, through 5.84×10^5 s for ZVI, to 1.69×10^7 s for Z. The breakthrough time for Ni was in the range of 8.16×10^6 s for MCA to 1.80×10^7 s for Z. Furthermore, the breakthrough time for Zn was in the range of 1.53×10^6 s for MCA to 5.08×10^7 s for Z. During the experiment, the concentration of Cd, Cu, Ni, Pb and Zn in the effluent solution from a column with layers of reactive materials and Cu, Zn for ZVI and Pb for column filled with Z was close to zero. The reduction of metal ions removal was due to high pH values of the solution (above 8.00). Therefore, MCA may be recomended as a "new" alternative reactive material for PRBs technology. The presented test results allow the conclusion that the PBR's layer system consisting of ZVI, Z and MCA for heavy metals removal is more effective than a single-layer system and is therefore more efficient on account of long-time effective cleaning without breakthrough times for contaminants.

Keywords: Permeable reactive barrier; Reactive materials; Heavy metals sorption; Zero-valent iron; Zeolite; Modified construction aggregate

1. Introduction

In recent years, there has been an increasing ecological concern related to environmental contamination by heavy metals, which are defined as metallic elements that have a relatively high density compared to water [1]. The natural sources such as erosion, weathering or volcanic eruptions have been reported to contribute to the heavy metal pollution

---

* Corresponding author.

of groundwater [1,2]. High concentrations of heavy metals are a result of human activities. The anthropogenic sources include agricultural, pharmaceutical, industrial production (e.g. metal processing in refineries, coal burning in power plants, petroleum combustion, nuclear power stations, plastics, textiles, microelectronics, and transport), wastewater and solid wastes [3–9]. Contaminants from sources mentioned above are deposited on the ground surface and with runoff may infiltrate as leachate into the groundwater causing its serious pollution because of their high bioavailability, toxicity and mobile nature [10,11]. Due to the fact that groundwater is a reservoir of fresh water (30% of the world's resources) and the main source of drinking water, the deterioration of their quality is one of the basic global environmental problems. This problem has attracted the attention of both research centers and international organizations such as the World Health Organization, the United Nations Educational, Scientific and Cultural Organization, the International Water Association and the Organization for Economic Co-operation and Development [12]. In many developed countries, a number of laws and regulations have been introduced to initiate actions aimed at minimizing pollutant emissions and improving the current quality status of groundwater. The implementation of these assumptions is based on the Water Framework Directive [13], introduced in the European Union, which sets limit values for priority substances, including heavy metals (cadmium, nickel, lead and mercury). In addition, according to its content, EU countries are obliged to achieve "good quality" of surface and groundwater.

In order to achieve this quality regulations, so far the high cost conventional techniques, such as impermeable barriers or "pump and treat" systems, were used for the remediation of contaminated groundwater [11,14]. However, difficulty and high costs of the aforementioned methods caused passive in situ remediation techniques to be favoured. These include permeable reactive barriers (PRBs), constructions that are semipermeable and permanent or replaceable [15–17]. These barriers capture the pollutants that flow through the saturated zone [15,18] and thus enhance the natural attenuation processes occurring in soil. The mobility of heavy metals dissolved in groundwater might be controlled by reactions that cause metals to be absorbed or to precipitate as well as by chemical reactions that keep metals associated with the solid phase of reactive materials filled with the PRBs [18]. Various low-cost materials, including agricultural and industrial wastes and local minerals, have been suggested for the removal of heavy metals, for example, peanut husk [19], rice husk, fly ash [20], charcoal [19], limestone [21], silica sand [22], bentonite, clay [23–25], diatomite [26], concrete [27] and modified minerals [19,28–30].

In PRB design, both laboratory batch and column tests are used to obtain information about intensity and kinetics of removal reactions between the contaminants in the solution and the reactive material [31–34]. In comparison, column tests are complicated and require more time but overcome some limitations of batch testing. Long-duration column experiments provide dynamic flow conditions that closely approximate those of a PRB in a field deployment (e.g. saturation of the reactive zone, flow velocity of the contaminated water, effective porosity and bulk density of reactive materials) [35,36].

The main objective of this study is to identify and test the transport mechanism of heavy metals (Cd, Cu, Ni, Pb and Zn) through zeolite (Z), zero-valent iron (ZVI), modified construction aggregate (MCA) and layered treatment zone of ZVI, Z and MCA, with the parameter evaluation of contaminant transport through porous materials using the STANMOD package CXTFIT [37]. Finally, the recommendation of the most favorable treatment media for the removal of heavy metals was made.

2. Experimental

2.1. Materials and chemicals

Materials for this study were chosen based on their availability, low cost and suspected or proven ability to remove heavy metals. Granular ZVI (iPutec GmbH & Co. KG, Rheinfelden, Germany), granular clinoptilolite-rich Slovak zeolite tuff – Z (Zeocem, Slovakia), and MCA (Wrzosówka Mine, Poland) met the above criteria and were used in laboratory tests as the reactive materials. The main fraction of rock materials from Wrzosówka Mine was spongolite and limestone. The material was prepared by using chemical deposition method. The surface of construction aggregate was immersed in 10% dose of aqueous solution of magnesium oxide (MgO) for half an hour in order to fully impregnate the pore of material. After that, MCA was dried at 120°C for 1 h and at 250°C for 1 h more. Subsequently, the impregnated sample was heated to 450°C for 4 h to increase the pore size and develop surface area by calcination. The modification of materials by MgO was performed in several studies [38–40]. The scanning electron images (QUANTA 250 FEG, FEI) and X-ray diffraction (XRD) patterns (X'pert APD, Philips) of the ZVI, zeolite and construction aggregate samples are shown in Fig. 1. The specific surface area was determined by Brunauer–Emmett–Tyller (BET) N_2 adsorption analysis, and the total pore volume was determined by Barret, Joyner Halendy adsorption analysis using the surface area analyser (ASAP 2020M, Micromeritics). The pattern of XRD and spectroscopy emission microscopy (SEM) images of the ZVI sample indicate that the dominant component is iron with the addition of silica, aluminium, magnesium and carbon. The S_{BET} of ZVI is 0.52 m^2/g and the total pore volume is 1.0×10^{-6} m^3/kg. The SEM image of the zeolite sample showed the microstructure of its surface and revealed that the main components are Si, Au, Al, Na and K. The pores have sizes from 0.1 to 10 μm and are irregular in shape. Its S_{BET} is 32.44 m^2/g and the total pore volume equals 5.0×10^{-6} m^3/kg [41]. In a diffraction pattern of the MCA, the strongest peaks were observed for calcite and quartz. The structure of the aggregate exhibits a rough and porous surface with MgO crystal aggregates. The specific surface area of the sample is 2.82 m^2/g and the total pore volume is 2.00×10^{-7} m^3/kg. The properties of the material (particle size distribution, specific gravity, bulk density, specific surface area and total pore volume) are summarized in Table 1.

In this study, the chemicals and reagents of analytical grade (CHEMPUR, Poland) and distilled water (DI) were used. The salts of heavy metals ($CdCl_2{\cdot}2.5H_2O$, $CuCl_2{\cdot}2H_2O$, $NiSO_4{\cdot}7H_2O$, $Pb(NO_3)_2$ and $ZnCl_2$) were diluted in DI and

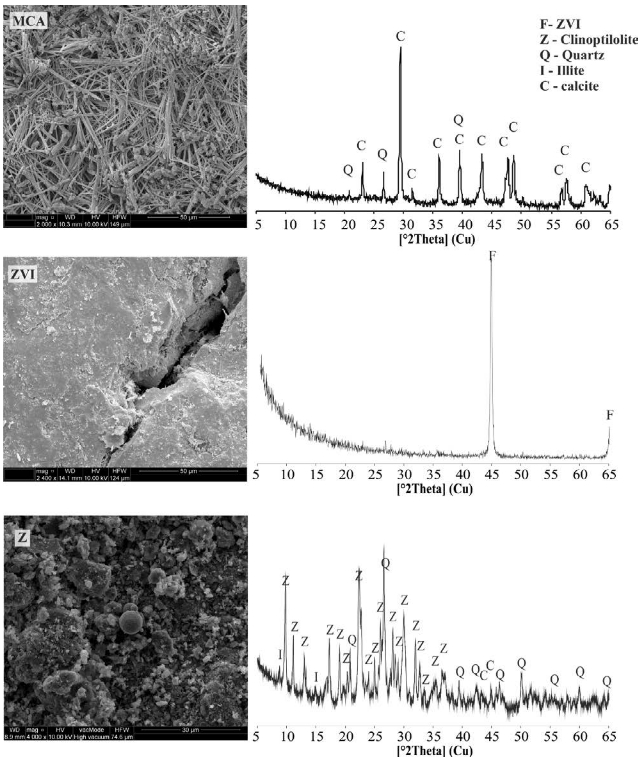

Fig. 1. SEM images and XRD patterns of modified construction aggregate, zero-valent iron and zeolite.

Table 1
Physical properties of the reactive materials

Material	Particle size (mm)	Specific gravity	Bulk density (cm^3/g)	Specific surface area (m^2/g)	Total pore volume (m^3/kg)
ZVI	0.5–2.0	7.61	6.700	0.52	1.0×10^{-6}
Zeolite	0.5–1.0	2.40	1.054	32.44	5.0×10^{-6}
Modified construction aggregate	0.5–2.0	2.71	1.820	2.82	2.0×10^{-7}

arranged according to our previous study [41]. The concentrations of 100 mg/L chloride solution using NaCl for column tests and 30 and 20 mg/L multicomponent solution of Cd, Cu, Ni, Pb and Zn for batch and column tests were used, respectively. Although the presence of chloride salts in the solution causes corrosion [42,43] of the ZVI bed, this process can have both positive and negative effects on water purification. During the corrosion of iron, an increase in the concentration of hydroxides and the associated precipitation of metals is observed, which is considered as one of the mechanisms for removing impurities. On the other hand, the occurrence of these processes (corrosion and precipitation of metals) results in a decrease in the porosity and hydraulic conductivity of the deposit. The use of the above chloride doses was dictated by their widespread use as de-icing agents in urban areas (e.g. highways, roads, gas stations, parking lots, landfills), where their concentrations often exceed acceptable standards [44,45]. In addition, the choice of chloride salts resulted from their use in earlier studies (batch, column and pilot type) over the use of ZVI in PBR technology [3–5].

The pH and electrical conductivity (EC) values were measured using a multiparameter instrument (YSI, USA). In the experiments, the pH of the chloride solution was in the range of 6.37–6.72 and the pH of the metal solution was between 5.50 and 6.00. Initial EC values ranged within 205–389 and within 45–57 mS/cm for the chloride and metal solutions, respectively.

2.1.1. Batch tests

Tests on heavy metals removal were conducted for the evaluation of a PRB system suitable for application in contaminated area such as industrial dumping and mining sites, brown fields or traffic infrastructure. The chemical compounds selected for testing were chosen based on several reports of the results of chemical composition analyses of the leachate from these sites [46,47]. In most cases, heavy metals concentrations that exceeded acceptable limits were observed. Therefore, the following ions of heavy metals were examined: Cd, Cu, Ni, Pb and Zn. The batch tests were the preliminary tests of heavy metals removal from an aqueous solution by selection of reactive materials. The tests were conducted as follows: in the first stage, 2.0 g of zeolite, ZVI and MCA were added to 100 mL of a solution (PE flask) with a constant concentration of heavy metals (30 mg/L); in the second stage, the flasks were sealed and placed in a rotary shaker at 15 rpm (GFL, Germany) at room temperature of 21°C ± 2°C. To determine the removal ratio changes in time span, the contents of flasks were agitated until the concentrations of metal ions were measured following 1, 3, 6, 10, 24 and 48 h. The content of metal in the solutions was determined by atomic absorption spectrometry – AAS method (Thermo Scientific iCE 3000, USA).

The removal ratio R_R (%) of metal by materials was calculated using the equation:

$$R_R(\%) = \frac{C_0 - C}{C_0} \times 100 \tag{1}$$

where C_0 and C are the initial and final metal concentrations (mg/L).

An additional control solution using DI water alone was used for two double-blind samples to measure background and residual metals within the testing equipment.

2.1.2. Column tests

Column tests were carried out with uni- and multi-compound solutions to evaluate the removal efficiencies by zeolite, ZVI and MCA. Laboratory-scale PRBs systems used in the experiment were designed using four PVC columns with 0.4 m length and 0.04 m internal diameter. The top and bottom of each column were sealed off with a PVC cap with a filter on the valve. The main parameters of the column tests are illustrated in Table 2.

Table 2
Column tests parameters

Column mark	Mass of dry material (g)	Porosity	Column PVF (mL)
MCA	2,649.4	0.21	103.08
ZVI	7,467.3	0.24	127.63
Z	2,355.0	0.47	260.16
ZVI	2,489.6	0.24	42.55
Z	785.16	0.47	76.92
MCA	883.3	0.21	34.38

The chemical solutions were continuously pumped into the column with downflow mode by a multichannel peristaltic pump (Zalimp, Poland) with a flow rates of 4.16×10^{-8} m^3/s in order to imitate real rates in the aquifer and replicate the performance of the PRB and of the pollutants in field conditions.

Performance comparison experiments were conducted using MCA alone, ZVI alone, zeolite alone (Z) and duplicate layers of ZVI, zeolite and MCA combined (Fig. 2). The columns filled with zeolite and ZVI alone were carried out due to its proven ability for the removal of heavy metals [48,49] and for comparison of the results in a test with a new material – MCA. Nowadays, the studies using ZVI as a comparison material are still performed by several researchers [50–52]. Moreover, ZVI is still the most popular reactive material used in PRB systems for groundwater remediation due to its reactivity and applicability for organic and inorganic contaminants removal [17,53–55]. However, the use of ZVI alone in most cases could reduce the permeability of barrier related to the decrease of pore volume of ZVI filter by mineral precipitates [54,56,57], by surface coating of ZVI particles and by gas formation in the PRBs [58]. Mineral precipitation in the ZVI is expected because corrosion causes an increase in pH value as a results of the reduction of aqueous protons [52,53]. Hence, the great need and high cost of standard reactive materials for water remediation created a requirement for low-cost alternative materials like recycled and/or rock materials. Selection and order of media were dictated by their removal properties. The first treatment layer from the bottom was ZVI, which was used to break down heavy metals by adsorption, reduction and coprecipitation. The middle layer was zeolite, which is well known for its cation exchange and adsorption properties. The third layer was MCA, which reveals high chemical precipitation capacity due to the increasing of pH in the solution. A recent review of literature shows that several laboratory studies on sequenced PRBs have been conducted using ZVI, zeolites, oxygen-release compound, lime stone and organic carbon (e.g. wood chips and compost) [59,60]. However, to our knowledge, the layers of ZVI, zeolite and MCA have never been performed in column tests. All materials were added to the columns in 5 cm lifts and compacted firmly with a pestle.

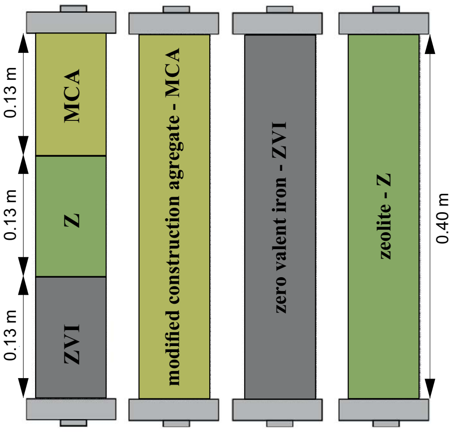

Fig. 2. Schematic diagram of the test columns columns test?

To ensure column saturation and minimize the occurrence of air bubbles entrapped in the material matrix, DI was fed up through the wing valve located at the bottom of a column from the bottom to the top of the samples. After saturation, the evaluation of hydrodynamic parameters of the reactive bed was performed by adding a pulse dose of chloride solution as a mobile tracer. The amount of adsorption was determined by conducting the column tests for a synthetic multicomponent model solution (20 mg/L of Cd, Cu, Ni, Pb and Zn).

At appropriate intervals, the effluent solutions from columns were collected for chemical analyses. The concentrations of metal ions were measured by atomic absorption spectrometry – AAS method (Thermo Scientific iCE 3000, USA), while the chloride ions were analyzed using the Mohr method. Solution pH and electrical conductivities were measured using multiparameter meter (YSI, USA). The experiments were performed at the constant temperature of the laboratory (20°C–22°C).

2.1.3. Hydrodynamic and sorption parameters

For estimating solute transport parameters (advection–dispersion) of selected contaminants through reactive materials, the software packages STANMOD and CXTFIT [37] were used. The parameters were calculated by applying a nonlinear least-squares parameter optimization method from the noticed column test data.

The following initial boundary assumptions were made in the developed numerical models: for the homogeneous sample, the initial concentration and diffusion coefficient D_M equal to zero. In this examination, the first-type (Dirac) boundary conditions and constant concentration of tested ions for the influent solution were assumed, while the zero-concentration gradient was estimated at the outlet of the column. The CXTFIT codes were used to estimate the following transport parameters from observed concentration distributions versus time: v_R ratio of flow velocity ($v_R = v/R$), D_R ratio of dispersion ($D_R = D/R$), α_L longitudinal dispersivity ($\alpha_L = D/v$), P_e Péclet number ($P_e = vL/D$), t_b breakthrough time, after which the mobile tracer concentration in the outlet was 0.5 C_0 and t_{bR} breakthrough time for a reactive tracer with retardation factor (the concentration in the outlet of the column was 0.95 C_0). Detailed description of the procedure used in the solution of advection–dispersion equation and calculation of transport parameters is presented by Toride et al. [37].

3. Results and discussion

3.1. Estimation of removal percentage of heavy metal—batch tests

The results for the removal of heavy metals with respect to contact time are shown in Fig. 3. From the zeolite graph,

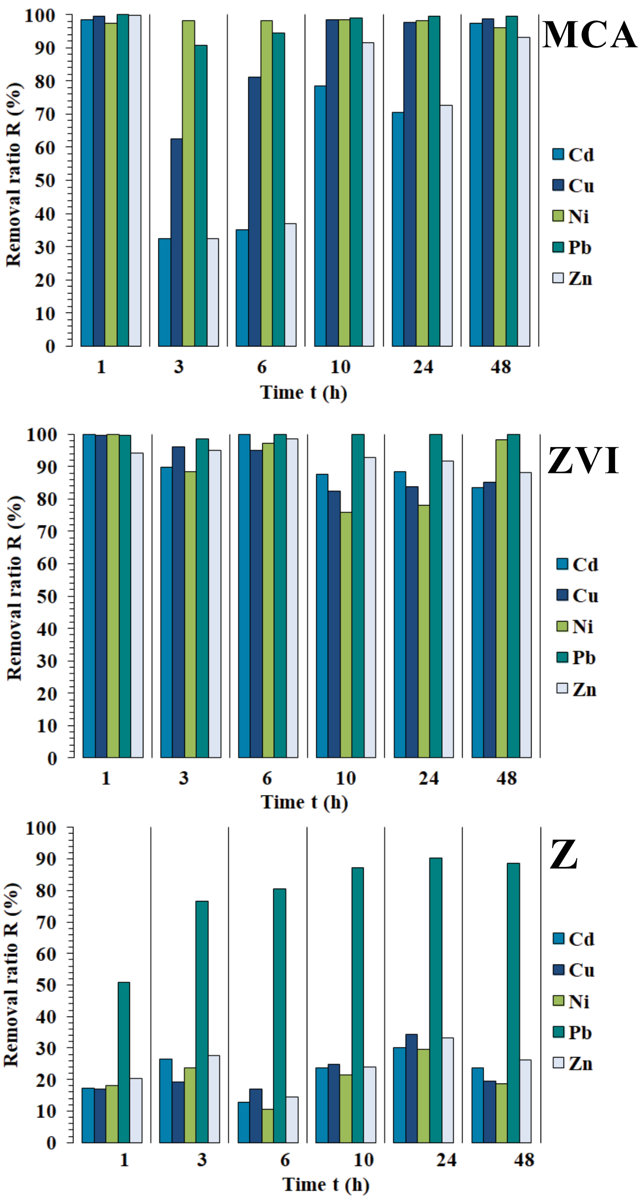

Fig. 3. The effect of removal ratio for MCA, ZVI, Z.

it can be concluded that the most intensive contaminants removal proceeded for lead ions. During the experiment, the removal of Pb was on average 88%, while for other metals was at approximately 20%. The component of the solution removed to the smallest extend by zeolite was nickel. Moreover, the percentage of metal ion adsorption on adsorbent is determined by the adsorption capacity of the adsorbent for various metal ions. From the values of the removal ratio, the order of adsorption priority on zeolite was as follows: Pb > Zn > Cd > Cu > Ni.

On the other hand, practically complete removal of heavy metals from the solution on ZVI was observed after the first hour of the experiment. At this time, the removal ratio was 99.85% for Cd, 99.62% for Cu, 99.83% for Ni, 99.80% for Pb and 94.13% for Zn. From the beginning to the end of the studies, the percentage removal of Ni and Pb show 100% removal, which indicates that these metals were the most favourable. The order of adsorption priority was the following: Pb > Zn > Cd > Ni > Cu.

The graph of alternative material and MCA shows that the material displayed high removal properties. The heavy metal removal expressed by *R* factor (%) revealed that from the aqueous solution Ni (98%) Pb (98%) and Cu (0.90%) were removed at the highest level, whereas the retardation factor of Zn and Cd during the contact time with MCA were 71% and 69%, respectively. The values of removal ratio indicated the following order of adsorption priority on MCA: Ni > Pb > Cu > Zn > Cd.

3.2. Test with mobile tracer – column tests

The measured breakthrough curves by the displacement experiments with a mobile tracer are shown in Fig. 4. In this figure, the relationships between the effluent concentration distributions versus the number of pore volume of flow (PVF), which represents the volume of the solutions equal to the volume of material pores, are presented. Moreover, the content of tracers in an outlet solution is presented as relative concentrations of chemicals C/C_0.

In this study, the backward analysis of the advection–dispersion equation was performed. The retardation coefficient *R* of chloride ions was assumed to be unity, and there was no interface between the contaminant and the material. In Table 3, the results of the calculation of transport parameters of the advection–dispersion equation are shown. In all analyses of the mobile tracer breakthrough curves, the equilibrium model was applied for zero-valent-iron, zeolite, MCA and layers of ZVI, Z and MCA. In Fig. 4, the fitted breakthrough curves for MCA and ZVI are regular and symmetrical. There is coherence between the ascent and descent with different times, which proves the homogeneity of the samples. However, there is a difference of the rise (prior) and fall (flattened, long and insignificantly disturbed tail) in Z and layers of ZVI, Z and MCA. The irregularities on the curve may be caused by a non-uniform particle size distribution of materials in columns. The values of transport parameters in CXTFIT were calculated with determination coefficients of 0.79–0.99, which predict good correlation to an exact match between observed and fitted data.

3.2. Test with reactive tracers – column tests

The breakthrough curves for reactive tracers are illustrated in Fig. 5. In general, the multi-layered column is more effective than a single one. This phenomenon was also confirmed in earlier studies using a system consisting of the following layers: raw construction aggregate, zeolite and activated carbon [41]. The presence of zeolite increased sorption impact on Cd and Pb, ZVI contributed to the increased removal capacity of Cu, Ni, Zn and MCA enhanced removal of Cu and Pb. Therefore, the final concentrations of Cd, Cu, Pb, and Zn in the effluent solution from multi-layered column were close to zero. In the graph in Fig. 5, Ni reduction can be observed, the course of which is less intense than other heavy metals in the solution.

The efficiency of heavy metals removal on ZVI was lesser, but still at a high level. The results showed that Cu, Ni and

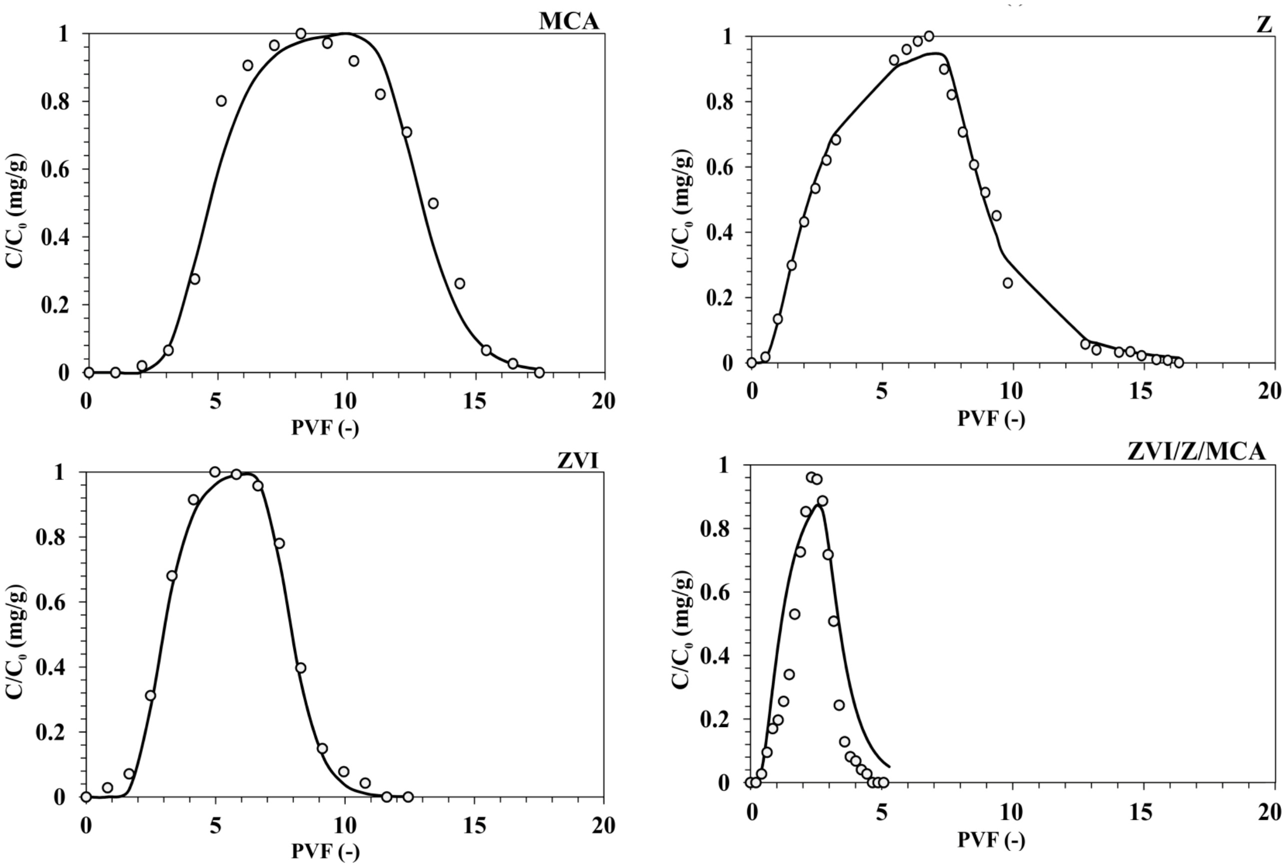

Fig. 4. Observed (circles) and fitted values (solid lines) of the mobile tracer for MCA, ZVI, Z and layers of ZVI, Z and MCA.

Table 3
Hydrodynamic and sorption parameters of MCA, ZVI, Z and layers of ZVI, Z and MCA obtained from column tests for the model solutions

Column	Amount of PVFs	v (m/s)	v_R (m/s)	D (m²/s)	D_R (m²/s)	R	α_L (m)	P_e	R^2
MCA Cl	1.03	3.90×10^{-5}	1	3.83×10^{-6}	1	1	0.10	10.20	0.97
MCA Cd	34.23	3.90×10^{-5}	1.70×10^{-7}	7.52×10^{-6}	3.30×10^{-6}	228	0.19	5.19	0.98
MCA Cu	34.23	3.90×10^{-5}	6.12×10^{-8}	1.51×10^{-4}	2.37×10^{-7}	637	3.39	0.26	0.88
MCA Ni	34.23	3.90×10^{-5}	6.13×10^{-6}	1.51×10^{-4}	2.37×10^{-9}	636	0.04	25.83	0.99
MCA Zn	34.23	3.90×10^{-5}	3.26×10^{-7}	3.55×10^{-5}	2.97×10^{-7}	120	0.91	1.10	0.96
ZVI Cl	0.83	4.95×10^{-5}	1	1.11×10^{-6}	1	1	0.23	44.47	0.99
ZVI Cd	14.38	4.95×10^{-5}	8.56×10^{-7}	2.60×10^{-6}	4.50×10^{-8}	58	0.05	19.04	0.99
ZVI Pb	14.38	4.95×10^{-5}	7.64×10^{-7}	5.11×10^{-6}	7.89×10^{-8}	650	0.10	9.69	0.98
Z Cl	0.53	6.01×10^{-5}	1	2.76×10^{-7}	1	1	0.01	217.75	0.92
Z Cd	27.78	3.18×10^{-5}	2.97×10^{-8}	3.14×10^{-7}	2.93×10^{-10}	1,072	0.01	40.46	0.99
Z Cu	27.78	3.18×10^{-5}	1.05×10^{-7}	3.70×10^{-8}	1.20×10^{-10}	302	0.01	340.51	0.98
Z Ni	27.78	3.18×10^{-5}	2.78×10^{-8}	1.67×10^{-5}	1.46×10^{-8}	1,144	0.52	0.76	0.98
Z Zn	27.78	3.18×10^{-5}	9.83×10^{-7}	1.30×10^{-6}	4.10×10^{-10}	3,234	0.04	9.69	0.98
ZVI,Z,MCACl	0.22	2.10×10^{-5}	1	1.11×10^{-4}	1	1	0.18	5.29	0.74

Note: PVF, the pore volume of flow; v, the velocity of flow; v_R, the ratio of decrease in flow velocity; D, the coefficient of hydrodynamic dispersion; D_R, the ratio of dispersion decrease; R, the retardation factor; α_L, the longitudinal dispersivity; P_e, the Péclet number.

Zn were removed at considerable extents, which was also noticed by Bilardi et al. [61]. In contrast, the concentrations of Cd and Pb ions decreased steeply in the beginning and then reached the breakthrough point. The low effluent Ni ($\leq C/C_0 = 0.2$) was continuously achieved during the entire operation period. The graphs of Cd and Pb (Fig. 5) show that the shape and gradient of the breakthrough curves were similar with changes of ion concentrations in the effluent

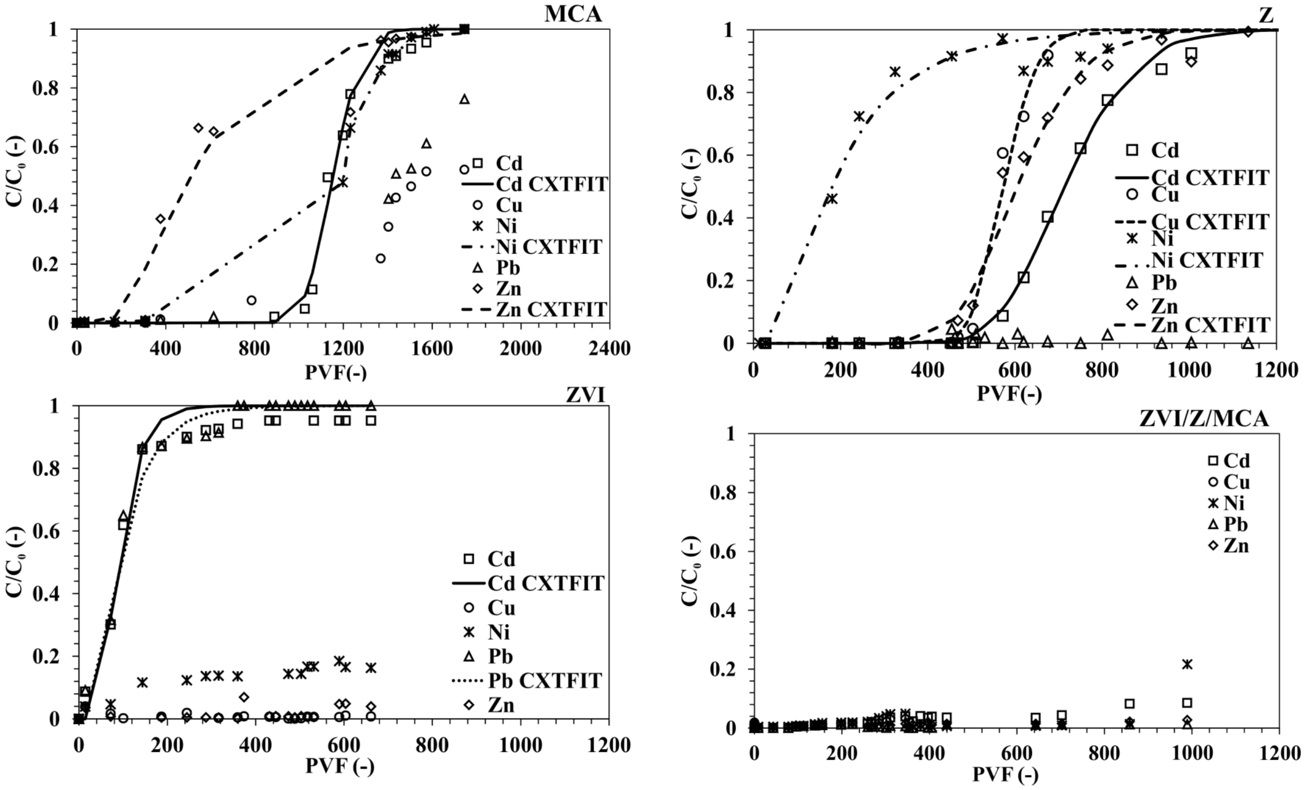

Fig. 5. Observed (points) and fitted values (lines) of the reactive indicators for MCA, ZVI, Z and layers of ZVI, Z and MCA.

solution. Literature presents studies on the use of ZVI to remove Cu from aqueous solutions by cementation process (i.e. reduction of the oxidized form of the contaminant, Cu^{2+}, and subsequent deposition of Cu^0 onto the iron surface) but also to adsorption and co-precipitation on iron corrosion products [62]. Moreover, the corrosion of Fe^0 and the subsequent increase of pH may also cause precipitation of $Fe(OH)_2$ at the start of the electrochemical process:

$$Fe^0 + 2H_2O \rightarrow Fe(OH)_2 + 2H^+ + 2e^- \tag{2}$$

The experiments of evaluating nickel removal by ZVI [55–57] indicated that spontaneous electrochemical cementation process between Ni and ZVI is less favourable than in the case of copper. The standard redox potential of the couple Ni^{2+}/Ni^0 is only marginally higher than that of Fe^{2+}/Fe^0 and consequently initiates removal by adsorption, co-precipitation and adsorptive size-exclusion. Otherwise, zinc reduction by ZVI is caused by lower standard redox potential of the couple Zn^{2+}/Zn^0 than of couple Fe^{2+}/Fe^0 due to other mechanisms activated by ZVI [63,64].

On the other hand, at the beginning, the increase in concentration of Ni and an earlier breakthrough point was observed in the column with zeolite. The increased concentration of Cd, Cu and Zn were detected in the outlet solution after time responding to PVF = 600. The shape of the breakthrough curves for Cd, Cu and Zn (Fig. 5) presented the same behaviour of ion concentrations during the entire experiment and evidenced their faster movement through the pore channels in diffusion processes [65]. The most immobilised ion during contact with zeolite was Pb and the final concentration in the outlet from the column was close to zero.

In the column with MCA, different intensities of heavy metals removal from the solution were observed. The most exhaustive removal was noticed for zinc as well as for cadmium and nickel. Lead and cooper ions were also immobilised, however, without achieving the equilibrium stage.

According to the characteristic points of the breakthrough curves (C/C_0 equal to 0.5 and 0.95), the dynamic sorption capacities S_m and S_{mR} of the materials were estimated. The calculated sorption parameters are presented in Table 4. The values of calculated S_{mR} were at a different level, which indicates diverse removal processes. The highest values were observed for Zn, Cd, Ni and Cu on zeolite – the material characterised by adsorption. Mean S_{mR} values were observed for Zn, Cd and Ni for MCA, while the lowest for Cd and Zn for ZVI. Moreover, referring to the values of R, the sorption processes were unlimited ($R > 1,000$) for Zn, Ni, Cd on zeolite, very high ($100 < R < 1,000$) for Cu on Z and for Cd, Cu, Ni, Pb, Zn on MCA, and high ($10 < R < 100$) for Pb and Cd on ZVI. In comparison to previous studies, the MCA was characterized by higher removal capacities than raw construction aggregate tested by Pawluk and Fronczyk [41]. The value of retardation factor was higher by one order of magnitude for MCA, whereas S_{mR} was more than five times smaller for a raw material.

In addition, the dispersivity estimated for tested reactive materials attained different values for individual heavy metals (Table 3), although, it is a physical parameter and should

Table 4
Hydraulic and sorption parameters of MCA, ZVI and Z obtained from column tests

Material	t_b (s)	t_{bR} (s)	S_m (mg/g)	S_{mR} (mg/g)
MCA Cd	1.28×10^4	2.93×10^6	2.341	3.590
MCA Cu	1.28×10^4	8.17×10^6	0.901	–
MCA Ni	1.28×10^4	8.16×10^6	2.731	3.590
MCA Pb	1.28×10^4	3.58×10^6	1.192	–
MCA Zn	1.28×10^4	1.53×10^6	0.878	4.487
ZVI Cd	1.01×10^4	5.84×10^5	0.055	0.273
ZVI Pb	1.01×10^4	6.55×10^5	0.011	0.240
Z Cd	1.57×10^4	1.69×10^7	6.094	11.034
Z Ni	1.57×10^4	1.80×10^7	1.405	7.957
Z Cu	1.57×10^4	4.75×10^6	5.932	7.957
Z Zn	1.57×10^4	5.08×10^7	5.446	11.839

Note: t_b, the breakthrough time for the mobile tracer that does not sorb to the material ($t_b = L/v$); t_{bR}, the breakthrough time for a tracer with retardation factor R ($t_{bR} = R \times t_b$); S_m and S_{mR}, the dynamic sorption capacities of the breakthrough points, at which the relative concentration of the tracer in the effluent solution is 0.5 and 0.95, respectively.

depend only on the properties of a porous material. However, according to Dufey et al. [66], the value of dispersivity may be affected by the chemical interactions between the solution and the material (e.g. dissolution and precipitation).

In the examination of the breakthrough capacity, several analogies were noticed: $S_{mR} = 11.839$ mg/g Zn, $S_{mR} = 11.034$ mg/g Cd, $S_{mR} = 7.957$ mg/g Ni and $S_{mR} = 7.957$ mg/g Cu for Z, $S_{mR} = 4.487$ mg/g Zn, $S_{mR} = 3.590$ mg/g Cd and Ni for MCA, $S_{mR} = 0.273$ mg/g Cd and $S_{mR} = 0.240$ mg/g Pb for ZVI. Having compared the estimated values of this parameter for all materials' beds, it was recognized that cadmium and zinc have a higher affinity to zeolite. In Table 3, the obtained retardation factors are presented. To compare the column system with numerical simulation (e.g. CXTFIT) for transport problems of contaminants, it is convenient to relate them by non-dimensional numbers like the Péclet number. The values of the Péclet number indicate the transport resulting mainly from the dispersion and advection mechanisms.

The pH and EC changes in the effluents solution in a function of time for columns filled with Z, MCA and ZVI and layers of ZVI, Z and MCA is shown in Fig. 6. The pH is one of the most important parameters for characterizing the chemical properties of aqueous solutions and controlling the adsorption behaviour. During the column experiments, the pH value of the effluent showed different removal processes of heavy metal ions from the solution – by sorption and precipitation. Observations indicated that in the first step of experiments, the initial pH increased to value of 10.40 for MCA, to 10.37 for a column with layers and to 10.40 for a zeolite bed, which pointed to precipitation of heavy metals. On the other hand, for a column with ZVI, pH was constant in the range of 4.60–5.26. Afterward, the reduction of pH to values in the range of 6.40 for the zeolite, and the value of about 8.77 for layered beds was observed. The results show clearly that the sorption on zeolites particles was a complex process. It is well known that heavy metals removal by zeolite is caused by ion exchange and surface complexation. On the other hand, the immobilization of heavy metal ions from aqueous solutions on MCA occurred mostly by precipitation and less by adsorption.

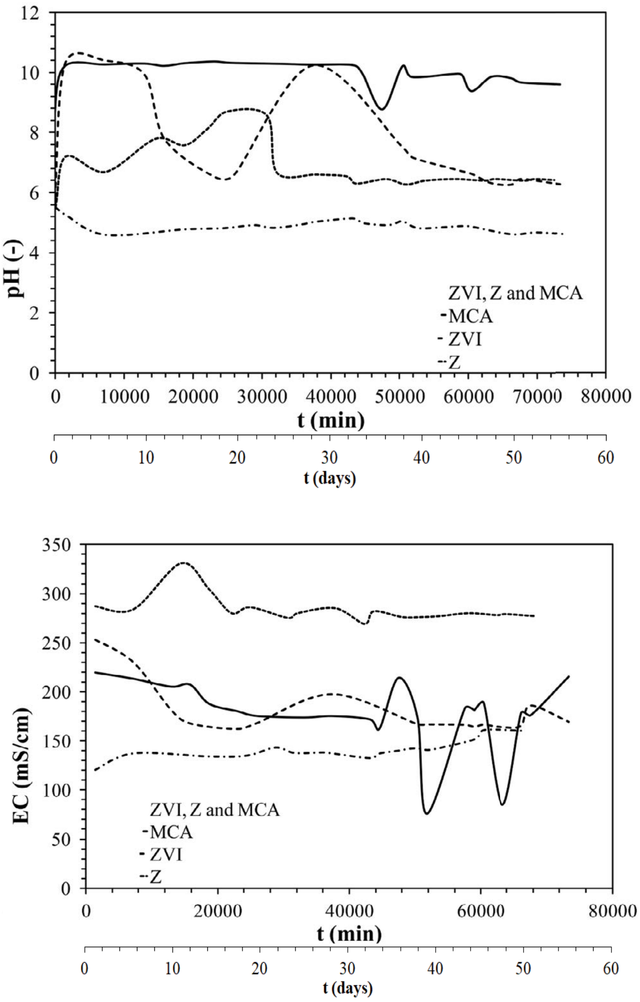

Fig. 6. The pH profile at the exit of the column with MCA, ZVI, zeolite and layers of ZVI, Z and MCA.

Moreover, the clogging of the ZVI beds was reported in the end of this experimental study. It was caused by cementation and precipitation processes on the material, especially during the contact with copper and nickel, which was observed as a blue precipitate. The decrease of the hydraulic conductivity of reactive materials mixture was also observed in the pilot-scale studies by Fronczyk [67].

4. Conclusions

In conclusion, the preliminary batch tests confirm the high efficiency of heavy metals removal from multicomponent solution during the contact with ZVI. Moreover, the high values of removal ratios for all tracers on MCA indicated the usefulness of this material for groundwater remediation. Column experiments with zeolite showed an earlier breakthrough point (tbR) for nickel, which had lower affinity for free place on the material surface than Cd, Cu and Zn ions. The highest removal on zeolite was found for lead ions and on ZVI for copper, nickel and zinc ions. The study carried out on the column with layered beds showed strong removal of all heavy metals from the multicomponent solution – the final concentrations of cadmium, copper, nickel, lead and zinc in the effluent solution from the column were close to zero. Based on the obtained results, cadmium was less effectively removed from the solution compared to the Cu, Ni, Pb and Zn ions during the contact with all the materials. On the modified material, the heavy metals were immobilized with different intensity. The most intensive reduction was noticed for Cu and Pb. On the other hand, maximum concentration of Cd, Ni and Zn was observed in effluent solution. The pH value of effluent during column tests showed that the ions of heavy metals were retained from the solution by both sorption and precipitation processes. The column tests showed that the multi-layered reactive zones are more efficient for heavy metal removal from multicomponent solution than single zones.

Acknowledgements

This work was supported by the National Science Centre, Poland under Grant No. N N523 561638. The authors declare that there is no conflict of interest.

References

[1] J.E. Fergusson, The Heavy Elements: Chemistry, Environmental Impact and Health Effects, Pergamon Press, Oxford, 1990.

[2] J.O. Nriagu, A global assessment of natural sources of atmospheric trace metals, Nature, 338 (1989) 47–49.

[3] O. Gibert, J.L. Cortina, J. de Pablo, C. Ayora, Performance of a field-scale permeable reactive barrier based on organic substrate and zero-valent iron for in situ remediation of acid mine drainage, Environ. Sci. Pollut. Res., 20 (2013) 7854–7862.

[4] E. Wołejko, B. Pawluśkiewicz, U. Wydro, T. Łoboda, A. Butarewicz, The effect of sewage sludge on the growth and species composition of the sward and the content of heavy metals in plants and urban soil, Ann. Warsaw Univ. Life Sci. – SGGW, Land Reclam., 46 (2014) 101–114.

[5] N. Feng, H. Ghoveisi, G. Bitton, J.-C.J. Bonzongo, Removal of phyto-accessible copper from contaminated soils using zero valent iron amendment and magnetic separation methods: assessment of residual toxicity using plant and MetPLATE™ studies, Environ. Pollut., 219 (2016) 9–18.

[6] M. Lech, J. Fronczyk, M. Radziemska, A. Sieczka, K. Garbulewski, E. Koda, Z. Lechowicz, Monitoring of total dissolved solids on agricultural lands using electrical conductivity measurements, Appl. Ecol. Environ. Res., 12 (2016) 285–295.

[7] D. Adamcová, M. Radziemska, A. Ridošková, S.A. Bartoň, P. Pelcová, J. Elbl, J. Kynický, M. Brtnický, M.D. Vaverková, Environmental assessment of the effects of a municipal landfill on the content and distribution of heavy metals in *Tanacetum vulgare* L., Chemosphere, 185 (2017) 1011–1018.

[8] E. Koda, A. Tkaczyk, M. Lech, P. Osinski, Application of electrical resistivity data sets for the evaluation of the pollution concentration level within landfill subsoil, Appl. Sci., 7 (2017) 262–275.

[9] A. Arruti, I. Fernández-Olmo, A. Irabien, Evaluation of the contribution of local sources to trace metals levels in urban PM2.5 and PM10 in the Cantabria region (Northern Spain), J. Environ. Monit., 12 (2010) 1451–1458.

[10] J.F. Peng, Y.H. Song, P. Yuan, X.Y. Cui, G.L. Qiu, The remediation of heavy metals contaminated sediment, J. Hazard. Mater., 161 (2009) 633–640.

[11] R.N. Yong, C.N. Mulligan, M. Fukue, Sustainable Practices in Geoenvironmental Engineering, CRC-Taylor & Fancis, Boca Raton, FL, 2015.

[12] S.B. Megdal, S. Eden, E. Shamir, Water governance, stakeholder engagement, and sustainable water resources management, Water, 9 (2017) 190.

[13] Directive 20000/60/EC of the European parliament and of the council of 23 Oct. 2000 establishing a framework for community action in the field of water policy, Ojec L 327/1 of 22.12.2000.

[14] S.S. Suthersan, Remediation Engineering: Design Concepts, CRC-Lewis Publishers, Boca Raton, FL, 1997.

[15] R.M. Powell, D. Blowes, R.W. Gillham, D. Schultz, T. Sivavec, R.W. Puls, R. Landis, Permeable Reactive Barrier Technologies for Contaminant Remediation, EPA/600/R–98/125, EPA, Washington, DC, 1998.

[16] A. Gavaskar, N. Gupta, B. Sass, R. Janosy, J. Hicks, Design Guidance for Application of Permeable Reactive Barriers for Groundwater Remediation, Battelle, Columbus, OH, 2000.

[17] F. Obiri-Nyarko, S. Johana Grajales-Mesa, G. Malina, An overview of permeable reactive barriers for in situ sustainable groundwater remediation, Chemosphere, 111 (2014) 243–259.

[18] A. Navarro, J.M. Chimenos, D. Muntaner, A.I. Fernandez, Permeable reactive barriers for removal of heavy metals: lab–scale experiments with low–grade magnesium oxide, Ground Water Monit. R., 26 (2006) 142–152.

[19] O.E.A. Salam, N.A. Reiad, M.M. ElShafei, A study of the removal characteristics of heavy metals from wastewater by low-cost adsorbents, J. Adv. Res., 2 (2011) 297–303.

[20] H.A. Hegazi, Removal of heavy metals from wastewater using agricultural and industrial wastes as adsorbents, HBRC J., 9 (2013) 276–282.

[21] A. Miller, L. Figueroa, T. Wildeman, Zinc and nickel removal in simulated limestone treatment of mining influenced water, Appl. Geochem., 26 (2011) 125–132.

[22] G. Bartzas, K. Komnitsas, Solid phase studies and geochemical modelling of low-cost permeable reactive barriers, J. Hazard. Mater., 183 (2010) 301–308.

[23] S. Babel, T.A. Kurniawan, Low-cost adsorbents for heavy metals uptake from contaminated water: a review, J. Hazard. Mater., 97 (2003) 219–243.

[24] M.Q. Jiang, Q.P. Wang, X.Y. Jin, Z.L. Chen, Removal of Pb (II) from aqueous solution using modified and unmodified kaolinite clay, J. Hazard. Mater., 170 (2009) 332–339.

[25] G. Varank, A. Demir, M.S. Bilgili, S. Top, E. Sekman, S. Yazici, H.S. Erkan, Equilibrium and kinetic studies on the removal of heavy metal ions with natural low-cost adsorbents, Environ. Prot. Eng., 40 (2014) 43–61.

[26] J. Liu, H.L. Wang, C.X. Lü, H.F. Liu, Z.X. Guo, C.L. Kang, Remove of heavy metals (Cu^{2+}, Pb^{2+}, Zn^{2+} and Cd^{2+}) in water through modified diatomite, Chem. Res. Chin. Univ., 29 (2013) 445–448.

[27] R.R. Holmes, M.L. Hart, J.T. Kevern, Heavy metal removal capacity of individual components of permeable reactive concrete, J. Contam. Hydrol., 196 (2017) 52–61.

[28] G. Chen, L. Shi, Removal of Cd (II) and Pb (II) ions from natural water using a low-cost synthetic mineral: behavior and mechanisms, RSC Adv., 7 (2017) 43445–43454.

[29] K.S. Shabani, F.D. Ardejani, K. Badii, M.E. Olya, Preparation and characterization of novel nano-mineral for the removal of several heavy metals from aqueous solution: Batch and continuous systems, A. J. Chem., 10 (2017) S3108–S3127.

[30] J. Yin, C. Deng, Z. Yu, X. Wang, Effective removal of lead ions from aqueous solution using nano illite/smectite clay: isotherm, kinetic, and thermodynamic modeling of adsorption, Water, 10 (2018) 210. doi:10.3390/w10020210

[31] Y.S. Ho, W.T. Chiu, C.C. Wang, Regression analysis for the sorption isotherm of basic dyes on sugarcane dust, Bioresour. Technol., 96 (2002) 1285–1291.

[32] X. Luo, H. Liu, G. Huang, Y. Li, Y. Zhao, X. Li, Remediation of arsenic-contaminated groundwater using media-injected permeable reactive barriers with a modified montmorillonite: sand tank studies, Environ. Sci. Pollut. Res., 23 (2016) 870–877.

[33] A. Gruszecka-Kosowska, P. Baran, M. Wdowin, W. Franus, Waste dolomite powder as an adsorbent of Cd, Pb(II), and Zn from aqueous solutions, Environ. Earth Sci., 76 (2017) 521.

[34] K. Pawluk, J. Fronczyk, K. Garbulewski, Reactivity of nano zero-valent iron (nZVI) in permeable reactive barriers (PRBs), Pol. J. Chem. Technol., 17 (2015) 7–10.

[35] T.A. Burt, Z. Li, R.S. Bowman, Evaluation of granular surfactant-modified/zeolite zero valent iron pellets as a reactive material for perchloroethylene reduction, J. Environ. Eng., 131 (2005) 934.

[36] F. Obiri-Nyarko, J. Kwiatkowska-Malina, G. Malina, T. Kasel, Geochemical modelling for predicting the long-term performance of zeolite-PRB to treat lead contaminated groundwater, J. Contam. H., 177–178 (2015) 76–84.

[37] N. Toride, F.J. Leij, M.Th. van Genuchten, The CXTFIT code for estimating transport parameters from laboratory or field tracer experiments, Version 2.1. Research Report No. 137, USDA-ARS U.S. Salinity Laboratory, Riverside, CA, 1999.

[38] Q. Liu, J. Ma, Y. Zhou, T. Wang, Synthesis of MgO-Modified mesoporous silica and its adsorption performance toward CO_2, Wuhan Univ. J. Nat. Sci., 19 (2014) 111–116.

[39] K. Zhou, L. Li, X. Ma, Y. Mo, R. Chen, H. Li, H. Li, Activated carbons modified by magnesium oxide as highly efficient sorbents for acetone, RSC Adv., 8 (2018) 2922–2932.

[40] A. Zukal, M. Kubů, J. Pastva, Two-dimensional zeolites: adsorption of carbon dioxide on pristine materials and on materials modified by magnesium oxide, J. CO2 Util., 21 (2017) 9–16.

[41] K. Pawluk, J. Fronczyk, Evaluation of single and multilayered reactive zones for heavy metals removal from stormwater, Environ. Technol., 36 (2015) 1576–1583.

[42] H. Ahn, H.Y. Jo, G.Y. Kim, Y.K. Koh, Effect of NaCl on Cr (VI) reduction by granular zero valent iron (ZVI) in aqueous solutions, Mater. Trans., 53 (2012) 1324–1329.

[43] M.G. Arroyo, V. Pérez-Herranz, M.T. Montanes, J. García-Antón, J.L. Guinon, Effect of pH and chloride concentration on the removal of hexavalent chromium in a batch electrocoagulation reactor, J. Hazard. Mater., 169 (2009) 1127–1133.

[44] E.V. Novotny, D. Murphy, H.G. Stefan, Increase of urban lake salinity by road deicing salt, Sci. Total Environ., 406 (2008) 131–144.

[45] M. Huber, A. Welker, B. Helmreich, Critical review of heavy metal pollution of traffic area runoff: occurrence, influencing factors, and partitioning, Sci. Total Environ., 541 (2016) 895–919.

[46] C. Zhao, C.-C. Wang, J.-Q. Li, C.-Y. Wang, Y.-R. Zhu, P. Wang, N. Zhang, Chemical characteristics of chromophoric dissolved organic matter in stormwater runoff of a typical residential area, Beijing, Desal. Water Treat., 57 (2016) 19727–19740.

[47] G. Tóth, T. Hermann, M.R. Da Silva, L. Montanarella, Heavy metals in agricultural soils of the European Union with implications for food safety, Environ. Int., 88 (2016) 299–309.

[48] M. Franus, M. Wdowin, L. Bandura, W. Franus, Removal of environmental pollutions using zeolites from fly ash: a review, Fresen. Environ. Bull., 24 (2015) 854–866.

[49] T.M. Statham, K.A. Mumford, S.C. Stark, D.B. Gore, G.W. Stevens, Removal of copper and zinc from ground water by granular zero-valent iron: a mechanistic study, Sep. Sci. Technol., 50 (2015) 1748–1756.

[50] L. Chen, Y. Liu, F. Xia, F. Liu, B. Li, Influences of benzene or toluene on dechlorination of perchloroethene and trichloroethene in a simulated zero-valent iron permeable reactive barrier, Water Qual. Res. J., 53 (2018) 61–71.

[51] H. Dong, Y. Chen, G. Sheng, J. Li, J. Cao, Z. Li, Y. Li, The roles of a pillared bentonite on enhancing Se (VI) removal by ZVI and the influence of co-existing solutes in groundwater, J. Hazard. Mater., 304 (2016) 306–312.

[52] S. Bilardi, P.S. Calabrò, R. Greco, N. Moraci, Removal of heavy metals from landfill leachate using zero valent iron and granular activated carbon, Environ. Technol., (2018) 1–13, https://doi.org/10.1080/09593330.2018.1503725.

[53] U. Santisukkasaem, D.B. Das, A non-dimensional analysis of permeability loss in zero-valent iron permeable reactive barrier (PRB), Transport Porous Med., (2018) 1–21, https://doi.org/10.1007/s11242-018-1096-0.

[54] K.E. Roehl, T. Meggyes, F.G. Simon, D.I. Stewart, Long-Term Performance of Permeable Reactive Barriers, 1st ed., Elsevier, Amsterdam, 2005.

[55] J. Vidal, C. Saez, P. Cañizares, V. Navarro, R. Salazar, M.A. Rodrigo, ZVI-reactive barriers for the remediation of soils polluted with Clopyralid: are they really worth? Chem. Eng. J., 350 (2018) 100–107.

[56] D. Phillips, T. Van Nooten, L. Bastiaens, M. Russell, K. Dickson, S. Plant, J. Ahad, T. Newton, T. Elliot, R. Kalin, Ten year performance evaluation of a field-scale zero-valent iron permeable reactive barrier installed to remediate trichloroethene contaminated groundwater, Environ. Sci. Technol., 44 (2010) 3861–3869.

[57] P. Luo, E.H. Bailey, S.J. Mooney, Quantification of changes in zero valent iron morphology using X-ray computed tomography, J. Environ. Sci., 25 (2013) 2344–235.

[58] N. Moraci, P.S. Calabrò, Heavy metals removal and hydraulic performance in zero-valent iron/pumice permeable reactive barriers, J. Environ. Manage., 91 (2010) 2336–2341.

[59] M. Barrett, P. Kearfott, J. Malina, Stormwater quality benefits of a porous friction course and its effect on pollutant removal by roadside shoulders, Water Environ. Res., 78 (2006) 2177–2185.

[60] X. Kong, E. Bi, F. Liu, G. Huang, J. Ma, Laboratory column study for evaluating a multimedia permeable reactive barrier for the remediation of ammonium contaminated groundwater, Environ Technol., 36 (2014) 1433–1440.

[61] S. Bilardi, P.S. Calabrò, S. Caré, N. Moraci, C. Noubactep, Improving the sustainability of granular iron/pumice systems for water treatment, J. Environ. Manage., 121 (2013) 133–141.

[62] Y. Ku, C.H. Chen, Kinetic study of copper deposition on iron by cementation reaction, Sep. Sci. Technol., 27 (1992) 1259–1275.

[63] J. Dries, L. Bastiaens, D. Springael, S.A. Agathos, L. Diels, Combined removal of chlorinated ethanes and heavy metals by zerovalent iron in batch and continuous flow column systems, Environ. Sci. Technol., 39 (2005) 8460–8465.

[64] G. Bartzas, K. Komnitsas, I. Paspaliaris, Laboratory evaluation of Fe0 barriers to treat acidic leachates, Miner. Eng., 19 (2006) 505–514.

[65] W. Jury, R. Horton, Soil Physics, 6th ed., John Wiley & Sons, INC., New York, 2004.

[66] J.E. Dufey, T.H. Sheta, G.R. Gobran, H. Laudelout, Dispersion of chloride, sodium, and calcium ions in soils affected by exchangeable sodium, Soil Sci. Soc. Am. J., 46 (1982) 47–50.

[67] J. Fronczyk, Artificial road runoff water treatment by a pilot-scale horizontal permeable treatment zone, Ecol. Eng., 107 (2017) 198–207.